



# Structure and local parameters of self-compressed plasma streams in external magnetic field

Yuliia Volkova ,  
Dmytro Solyakov ,  
Anna Marchenko ,  
Volodymyr Chebotarev,  
Igor Garkusha ,  
Vadym Makhlai ,  
Maryna Ladygina ,  
Tetyana Merenkova ,  
Dmytro Yeliseyev,  
Yurii Petrov ,  
Valerii Staltsov

**Abstract.** The influence of the external axial magnetic field on pinching plasma flows generated by a magneto-plasma compressor (MPC) has been studied using magnetic and electric probes. In the presence of an external magnetic field, temperature measurements show two groups of electrons with different temperatures near the plasma stream core. The external magnetic field leads to a noticeable increase in the electric current in the plasma stream, electron temperature, and the formation of the current-sheet-like structure observed in the MPC for the first time.

**Keywords:** Current sheet • Electric probe • Electron temperature • Drift velocity • Pinching discharge • Plasma accelerators

Y. Volkova<sup>✉</sup>, I. Garkusha  
Institute of Plasma Physics National Science Center  
“Kharkiv Institute of Physics and Technology”  
Kharkiv, Ukraine  
and V. N. Karazin Kharkiv National University  
Kharkiv, Ukraine  
E-mail: y.e.volkova.kh@gmail.com

D. Solyakov, V. Chebotarev, V. Makhlai, T. Merenkova,  
D. Yeliseyev, Y. Petrov, V. Staltsov  
Institute of Plasma Physics National Science Center  
“Kharkiv Institute of Physics and Technology”  
Kharkiv, Ukraine

A. Marchenko, M. Ladygina  
Institute of Plasma Physics National Science Center  
“Kharkiv Institute of Physics and Technology”  
Kharkiv, Ukraine  
and Institute of Plasma Physics and Laser Microfusion  
Hery 23 St., 01-497 Warsaw, Poland

Received: 22 September 2022

Accepted: 24 November 2022

0029-5922 © 2023 The Author(s). Published by the Institute of Nuclear Chemistry and Technology.  
This is an open access article under the CC BY-NC-ND 4.0 licence (<http://creativecommons.org/licenses/by-nc-nd/4.0/>).

## Introduction

Different modifications of high-current plasmadynamic systems, such as quasistationary plasma accelerators (QSPA) and magnetoplasma compressors (MPC), which operate in a quasistationary mode and are able to generate powerful plasma streams, have been studied for a long time. Such streams are widely used to solve important problems in various fields of science and technology: filling magnetic plasma traps of different configurations with working substances, testing the performance of materials in conditions reproducing the extreme plasma loads in thermonuclear reactors [1], and modifying and improving surface properties of materials [2, 3], as well as in the development of new generation devices for lithography [4]. The MPC, used in the present research, is a type of quasistationary plasma device that generates plasma streams with a pronounced pinching effect [4–9]. Previously, MPC plasma streams with a plasma density of  $10^{18} \text{ cm}^{-3}$  [5, 7, 8], a temperature of a 100 eV [7], and a velocity of  $10^7 \text{ cm/s}$  [6, 7] were obtained. However, in the process of plasma acceleration in the discharge channel, there is a dearth in the number of current carriers in the anode zone, which, consequently, leads to a transition of the plasmadynamic device to the “current crisis” mode and further deterioration of plasma flow parameters. One of the straightforward ways to

overcome the “current crisis” is to use an external axial magnetic field in the accelerating channel [10, 11]. Even though many studies regarding the generation of plasma flows in profiled channels have been conducted over the decades, the scientific literature reports only some particular aspects of the dynamics of high-energy plasma streams in profiled channels in the presence of an external magnetic field [10, 11]. No systematic experimental investigations were performed up to now to analyze these issues. Our first experimental studies with the MPC operating in the external axial magnetic field are available in the literature [11, 12]. Earlier experiments have shown that the plasma flow generated by the MPC has a rather complex spatial structure. There are local areas of plasma compression, toroidal vortices of electric current, closed contours of electric potential, and so-called zones of reverse flow formed in the plasma streams [5, 7, 8, 11]. All this imposes additional requirements on the methods used to determine different plasma parameters. Widely employed optical techniques allow us to obtain the data averaged along the line of sight, yet they do not make it possible to reveal the intricate structure of individual layers of plasma flow. More importantly, the ratio of the intensities of different spectral lines or the pressure balance equation used previously [6, 7] for electron temperature measurements cannot give its local value, especially, in the near-axis region where the compression zone forms. In order to be able to conduct local measurements, we have designed a set of magnetic and double electric probes [11, 12]. Double electric probes are very useful for measurements of the electron temperature with good temporal and spatial resolution in various devices [13–16]. The advantage of a double probe is that it does not require a reference electrode, decreases plasma perturbations, and limits collected current to the ion saturation current [16]. Nevertheless, the possible local disturbances of plasma introduced by probes should be precisely analyzed. We have shown earlier that the double probe operates in the diffusion regime at a range of plasma parameters typical for the MPC discharge [12]. However, the value of the ion saturation current measured by the probe turned out to be lower than Langmuir’s current due to the attenuation in the near-probe sheath. Such attenuation was also reported in certain studies [14, 15], although other studies suggest that the apparent electron temperature might be overestimated [16]. In the case when the electron energy distribution function (EEDF) is bi-Maxwellian with two well-separated temperatures [17], the results can be obtained by straight-line fits on the semi-logarithmic current–voltage characteristic. The two-temperature Maxwellian EEDF near the compression zone of the MPC plasma streams has been discovered for the first time in our previous experiments [12].

Concerning the plasma stream behavior in the external magnetic field, it is essential to measure local magnetic and electric fields and obtain two-dimensional distributions of electric currents and drift velocities. In our first study, special attention was paid to the most important stage of the plasma lifetime

corresponding to the first half-period of the discharge current [11]. We have shown that the external magnetic field leads to an increase in the magnitude of the self-generated magnetic field and changes the spatial distribution of the electric current.

In this paper, we report the outcomes of our recent experiments on the influence of the external magnetic field on the local electron temperature, plasma stream structure, and dynamics. This paper is structured as follows: the first section describes the experimental setup and diagnostics system. The second and third sections present the experimental results and discussion of the findings, respectively. The last section explains the conclusions.

### Experimental facility MPC

Experiments have been performed in the MPC device described in the literature [4–8]. The MPC is installed in the vacuum chamber with a diameter of 40 cm and length of 2 m. A system of capacitor banks with the total capacitance of 90  $\mu$ F triggered by a vacuum spark gap supplies the MPC discharge. The MPC device operates in a regime with residual gas at different pressures. The Rogowski coil and high-voltage dividers are used to measure the total discharge current and voltage. We applied magnetic field probes for the measurements of the self-generated magnetic field  $B_\phi$  in the plasma streams outside the MPC accelerating channel at different distances from the MPC outlet and radii. Each magnetic probe is a small cylindrical coil (5 mm in diameter) shielded by a ceramic case [11]. A set of electric probes was used for the measurements of the local electron temperature and radial component of the electric field. The magnetic coil installed on the MPC [11, 12] produces an axial magnetic field of up to 0.4 T inside the channel. The magnetic coil is 17 cm in length and 15 cm in diameter. The external magnetic field is applied only inside the accelerator and is negligibly small outside of it [11]. The average error of the probe measurements accounted for up to 15%. A picture of the magnetic-coil-installed MPC channel inside the vacuum vessel is shown in Fig. 1. The graph below illustrates the scale of the system. For all measurements discussed below, zero on the horizontal  $z$ -axis equals the cathode outlet.

### Electric probes measurements

The double probe we used for the measurements of the electron temperature consists of two cylindrical probes (pins) made of molybdenum wire disposed at the distance of about 6 mm one to the other. Each pin of the probe is fixed in a ceramic shield, leaving only the active part (3 mm) non-isolated. The results of the double electric probe measurements should be interpreted with respect to the regime of operation that depends on plasma density, temperature, density of neutral atoms, and magnetic field magnitude. As has been noted above, under the conditions of the MPC discharge, a double cylindrical probe

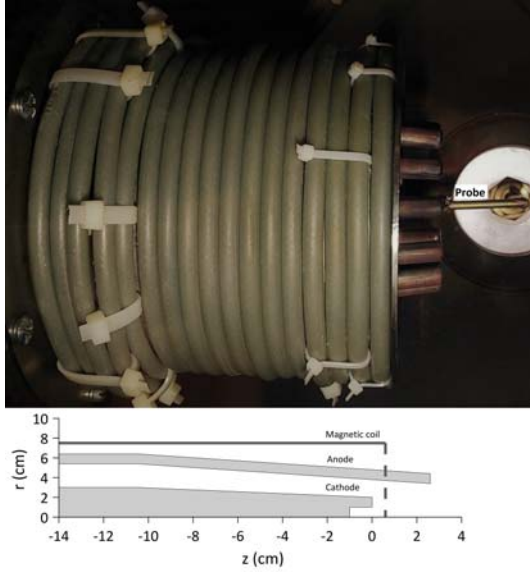


**Fig. 1.** The MPC accelerator with the magnetic coil and probe installed inside the vacuum chamber.

operates in the diffusion regime typical for dense plasma [13–16]. In this case, the mean free path ( $\lambda$ ) is much smaller than the probe radius ( $R_p$ ) and ionization length ( $L_i$ ). Additionally, if the  $L_i \gg R_p$ , as in the MPC plasma, the ion saturation current does not depend on the probe radius. The latter allows one to determine the regime of operation, which we have done in our preliminary experiments with the probe consisting of pins of different diameters of the working part, namely 1 mm and 0.3 mm [12]. The power to the probe is supplied by the isolated capacitor bank of 0.05 F (with a maximum voltage of up to 100 V) connected between two pins outside the MPC vacuum chamber. The measuring circuit is isolated from the MPC accelerating system and plasma by a sensitive Rogowski coil. For the measurements, the double probe is introduced inside the vacuum chamber of the MPC device and oriented radially. The experiments have been carried out in the MPC facility under the following conditions: the pressure of the residual gas helium of 2 Torr; the discharge current  $I_d = 400$  kA; and the magnitude of the external axial magnetic field ( $B_z$ ) inside the MPC channel of 0 T and 0.24 T. The local electron temperature can be determined from the current–voltage (I–V) characteristic of the double electric probe measured at different spatial positions inside the vacuum chamber during the discharge. Figure 2 shows the typical signals of the double probe and discharge current for three consecutive MPC shots. As can be observed, the signals of the probe are reproducible with respect to the discharge current and duration.

The temperature measurements have been performed for 8  $\mu$ s, 10  $\mu$ s, and 16  $\mu$ s of the MPC discharge time, at different distances from the MPC output at the radius of 2 cm from the center of the plasma stream. This radius was chosen as the typical radius of the compression zone and is of great importance for the determination of the influence of the external magnetic field on the processes in its vicinity. The electric probe measurements are rather complicated at smaller radii due to the rapid irradiation

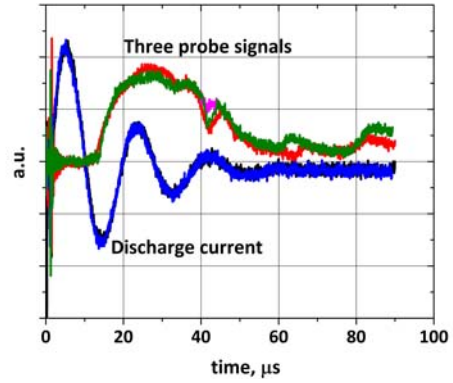


**Fig. 2.** The double probe and discharge current signals for three consecutive MPC shots.

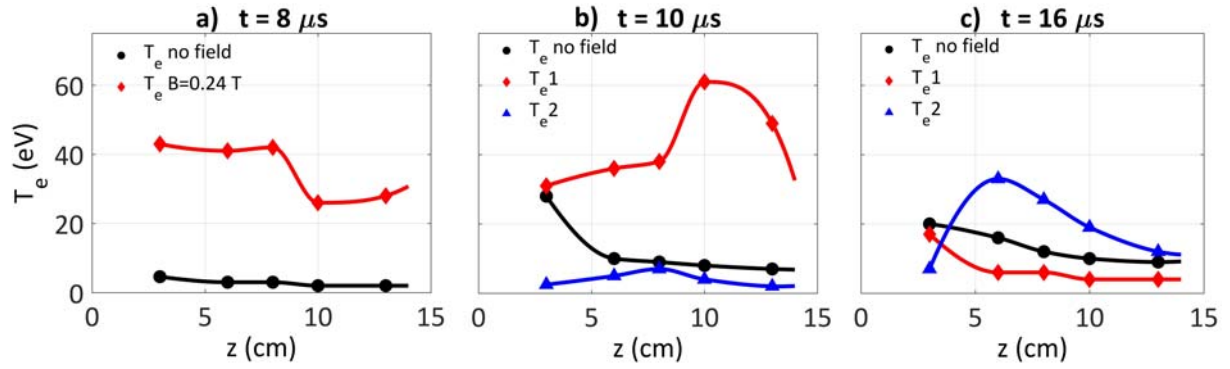
tion and further evaporation of its pins associated with the high temperature reached inside the region of the compression. The electron temperature can be obtained from Langmuir’s theory by assuming the EEFD to be close to Maxwellian, the ion current independent of voltage, and both tips operating in the collisionless regime:

$$(1) \quad T_e = \frac{1}{2} I_{\text{saturation}} \cdot \left[ \frac{dI}{dU} \right]_{U_p \rightarrow 0}^{-1}$$

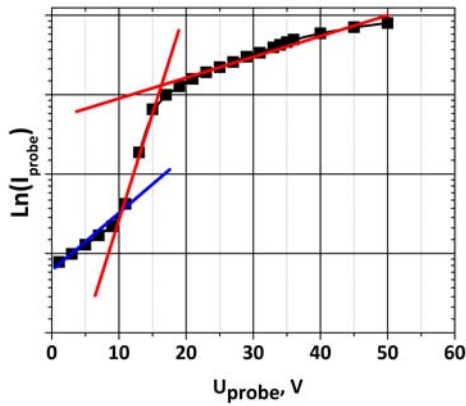
where  $I_{\text{saturation}}$  represents the ion saturation current, and  $U_p$  the probe biasing voltage. The measurements of the electron temperature with double probes have been interpreted with a number of assumptions, which inevitably affect the accuracy of the obtained results. As has been mentioned above, the apparent electron temperature is underestimated in this case due to the attenuation of the ion saturation current in the near-probe sheath. The reduction ratio changes with the probe position and is found to be small in the periphery region of the plasma stream [12], although, unfortunately, it is not possible to determine the attenuation coefficient due to the diagnostic limitations of the current research. Nevertheless, this approach allows us to estimate the lower level of the local electron temperature in different parts of the plasma stream.

Figure 3a shows the electron temperature distribution along the distance from the MPC output measured for the 8  $\mu$ s at the radius of 2 cm from the center of the plasma stream, at the presence of the external magnetic field of 0.24 T and without it. This moment of the discharge is characterized as the initial development of the plasma flow when the compression zone is not formed yet, and thus, the temperature in its vicinity has not yet achieved its maximum and is typically quite low (about 3 eV) without the external field. It is clearly seen that the application of the external B-field increases the temperature along the entire length of the stream. The resultant increase is greater at the distances closer to the MPC output (3–8 cm) and is approximately tenfold (from 4 eV to about 40 eV). This can be explained by a more pronounced influence of the B-field due to the proximity of the magnetic coil.

Even at the presence of the external B-field, the temperature drops down along the length of stream. As for the temperature dependences later during



**Fig. 3.** The electron temperature vs. distance from the MPC output measured at the radius of 2 cm from the center of the plasma stream for three moments of the discharge: (a) 8  $\mu$ s, (b) 10  $\mu$ s, and (c) 16  $\mu$ s.



**Fig. 4.** Double probe I–V curve plotted semi-logarithmically vs. the probe voltage where the transition region consists of two linear segments indicating the presence of two groups of electrons.

the discharge (Figs. 3b and 3c), the trend remains similar: the presence of the external field leads to its significant growth. When there is no magnetic field, the temperature peaks at the typical location of the compression (8 cm) and gradually decreases along the distance. With the B-field applied, however, the transition region of the probe I–V curve (Fig. 4) consists of two linear segments indicating the bi-Maxwellian EEDF. This unusual finding points to the presence of two populations of electrons near the compression zone. At 10  $\mu$ s of the discharge (Fig. 3b), the second temperature corresponding to the second group of electrons reaches a peak of slightly over 60 eV at the distance of 10 cm, whereas the first temperature corresponding to the first group of electrons stays relatively low, except the region of the accelerators output (3 cm). Notably, in our previous study [11], the currents distribution for this moment of the discharge pointed to the location of the compression zone at a distance of 7–14 cm. This can serve as an explanation for the fact that the temperature peak is shifted and, probably, means that the compression zone forms farther than usual. Surprisingly, 6  $\mu$ s later (Fig. 3c), these two groups of electrons switched tendencies: the second one reaches a peak at the typical distance of the compression region (5–8 cm) and is three times as high as it is at 10  $\mu$ s. At the same time, the first temperature goes down significantly, reaching only 4 eV at 10 cm, and is even lower than in the case when no magnetic field is applied.



**Fig. 5.** The probe used for the measurements of the electric field radial component.

The electric probe of a slightly different design was applied in order to conduct measurements of the radial component of the electric field in plasma. Magnitude can be obtained by dividing the measured potential difference by the distance between the pins of the probe. This probe consists of two molybdenum cylindrical electrodes of the same size (approximately 1 mm in diameter) placed at a radius of 1 cm from each other. Each of the electrodes has a protective ceramic tube. The distance between the ceramic tubes is around 6 mm. The measuring circuit of the electric probe consists of a voltage divider and a 10 kV isolation transformer. A picture of the electric probe measuring the radial component of the electric field is shown in Fig. 5. These measurements were used for the calculations of the drift velocities presented in the forthcoming section of this paper.

### Distributions of electric current and drift velocity in MPC plasma streams

The two-dimensional distributions of electric current and drift velocity are used to trace the dynamics of the plasma flow and changes in its structure. The drift velocities distribution was obtained from the measurements of the electric and magnetic fields performed with the double electric and magnetic probes described in the previous sections. The electric current distributions were plotted using the data from the magnetic probe measurements of the self-generated magnetic field outside the accelerating channel. Since the measurements at radii smaller than 1 cm are difficult, the data for the near-axis region were extrapolated, assuming the axial symmetry of the plasma stream and the fact that the magnetic field is close to 0 T on the axis itself. The results were obtained for the discharge time of 8  $\mu$ s and 16  $\mu$ s, in the presence of the external magnetic field of 0.24 T and without it. The following figures illustrate only the direction of the drift velocity. The cath-

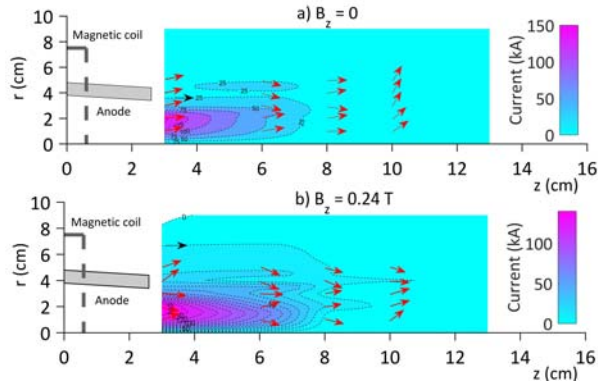


**Fig. 6.** Distributions of the electric current and drift velocity without (a) and with an external B-field (b) at  $8 \mu\text{s}$  of the discharge. The black arrows indicate the direction of the current flow; the red arrows depict the direction of the drift velocity.

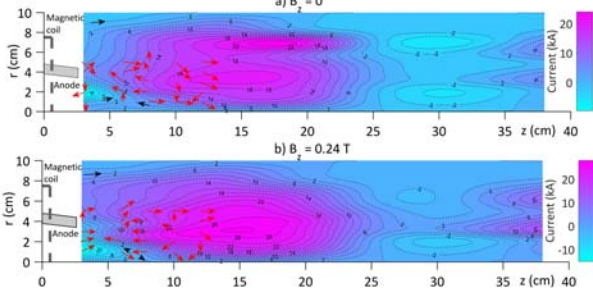


**Fig. 7.** Distributions of the electric current and drift velocity without (a) and with an external B-field (b) at  $16 \mu\text{s}$  of the discharge. The black arrows indicate the direction of the current flow; the red arrows depict the direction of the drift velocity.

ode outlet is set as a zero reference for the horizontal axis (see Fig. 1). Figure 6 illustrates the distributions of the current isolines and drift velocity in the plasma flows outside the MPC accelerating channel for the discharge time of  $8 \mu\text{s}$ . As mentioned above, at this moment of the discharge, no compression zone is formed yet. Without the external magnetic field (Fig. 6a), the current magnitude is greater closer to the electrodes, reaching as high as 125 kA, and decreases with the distance. The drift velocity direction coincides with the direction of the flow propagation, excluding the cross-section at 9 cm, where it points toward the wall of the vacuum vessel. This might be related to the divergence of the head part of the stream (taking into account the stream axial symmetry) and subsequent motion of the remaining plasma to the periphery. As for the external B-field influence (Fig. 6b), the electric current increases to nearly 140 kA. In the vicinity of the accelerator, both the drift velocity direction and location of the current vortices imply that the plasma flow increases in volume.

Later during the discharge, at  $16 \mu\text{s}$ , the impact of the external B-field becomes even more considerable (Figs. 7a and 7b). In its absence, the current distribution illustrates the grown complexity of the plasma stream structure: the numerous current vortices occupy most of the plasma stream volume approaching the chamber wall, while the current of

the reverse flow appears nearby the electrodes. The latter phenomenon has not been studied yet and is only observed during the later stages of the plasma stream lifetime, preceding its following disruption. The drift velocity at this location is directed to the accelerator as well, which might mean that the tail layers of the stream flow back to the output and can be damaging to the electrodes. A small near-axis volume (about 1 cm in radius) at the distance from 5 cm to 9 cm is surrounded by the current isolines pushed out of the center of the stream and vortices forming above it. Such a configuration of the currents is usually associated with the decay of the compression zone, which is typically less pronounced at this stage of the discharge.

Considering the external B-field influence (Fig. 7b), the number of current vortices decreases, although the current magnitude goes up slightly and the current of the opposite direction is still present right near the MPC output. The formation of the current vortices is thought to be a result of the conversion of the thermal and kinetic energy into the magnetic field energy, which should decrease the compression parameters. Conversely, fewer vortices possibly means that the compression mode is more pronounced, and its parameters should improve. The observed increase of the electron temperature for this case justifies such a conclusion. Apart from that, the layer surrounded by oppositely directed currents and drift velocities appears between 6 cm and 8 cm. As shown in Fig. 3c, there are two groups of electrons of different temperatures present at this moment of the discharge, and the second one goes up at the same distance where the layer forms. To illustrate the process in detail, we plotted a qualitative diagram (Fig. 8), which shows the behavior of current, magnetic field, temperature, and drift velocity at this specific layer, according to the measurements conducted.

The current density reaches a peak at the location of the stream where the magnetic field reverses direction. All this may point to the formation of

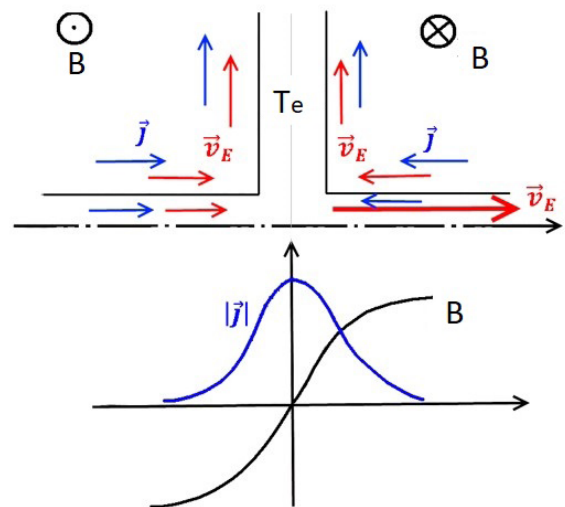


**Fig. 8.** The illustration of the behavior of current density, magnetic field, temperature, and drift velocity near the center of the plasma stream at the distance of 6–8 cm.

a current-sheet-like structure. The fact that the temperature reaches a peak at this particular location might be attributed to a supposed outflow of electron jets from the layer. Since it has been discovered in the MPC plasma streams for the first time, these observations are to be explored in more detail in our future research.









## Conclusions

We have studied the effect of the external magnetic field on the structure, dynamics, and local parameters of self-compressed plasma flows. A set of magnetic and electric probes has been developed to measure the self-generated magnetic field, electron temperature, and electric field locally with sufficiently high temporal and spatial resolution. When an external B-field is applied inside the MPC channel, the probe I-V characteristic indicates the presence of two populations of electrons of different temperatures in the vicinity of the center of the plasma stream, where the compression zone is formed. The external magnetic field generally leads not only to the bi-Maxwellian EEDF but also to a noticeable increase in the electron temperature. The two-dimensional distributions of drift velocity and the electric current isolines were plotted to obtain a detailed presentation of the plasma stream structure and its behavior during the discharge. Plasma flow has a rather complex structure: local compression region, toroidal current vortices, return currents, etc. The sets of concentric vortices and enclosed toroidal current structures are observed throughout the entire lifetime of the plasma stream. The electric current in the plasma stream, which normally flows from the anode to the cathode, changes its direction near the electrodes the second half-period of the discharge current. We found that the external magnetic field leads to the overall increase in the electric current magnitude and the formation of fewer current vortices at the later stages of the discharge. Furthermore, a current-sheet-like structure is formed in close proximity to the core of the plasma stream. It has not been observed previously in the MPC discharge and requires comprehensive research in the future. This result is promising as, if confirmed, it opens an opportunity to study the phenomena found in space plasma during solar flares and coronal mass ejections under laboratory conditions.

**Acknowledgments.** This work has been supported by the Targeted Program of the National Academy of Sciences of Ukraine (NASU) on Plasma Physics No. П-9/24-2020. This work has been carried out within the framework of the EUROfusion Consortium, funded by the European Union via the Euratom Research and Training Programme (Grant Agreement No. 101052200 – EUROfusion). Views and opinions expressed are however those of the author(s) only and do not necessarily reflect those of the European Union or the European Commission. Neither the European

Union nor the European Commission can be held responsible for them.

## ORCID

I. Garkusha  <http://orcid.org/0000-0001-6538-6862>  
 M. Ladygina  <http://orcid.org/0000-0001-7401-7778>  
 V. Makhlay  <http://orcid.org/0000-0002-5258-7793>  
 A. Marchenko  <http://orcid.org/0000-0002-2006-7080>  
 T. Merenkova  <http://orcid.org/0000-0002-1692-9354>  
 Y. Petrov  <http://orcid.org/0000-0002-4796-3002>  
 D. Solyakov  <http://orcid.org/0000-0001-5616-7078>  
 Y. Volkova  <http://orcid.org/0000-0003-4311-3681>

## References

- Garkusha, I. E., Makhlay, V. A., Petrov, Yu. V., Herashchenko, S. S., Ladygina, M. S., Aksenov, N. N., Byrka, O. V., Chebotarev, V. V., Kulik, N. V., Staltsov, V. V., & Pestchanyi, S. (2021). Vapour shielding of liquid-metal CPS-based targets under ELM-like and disruption transient loading. *Nucl. Fusion*, *61*, 116040. DOI: 10.1088/1741-4326/ac26ec.
- Zdunek, K. (1995). Spreading of impulse plasma within a coaxial accelerator. *Surf. Coat. Technol.*, *74/75*, 949–952. DOI: 10.1016/0257-8972(95)80038-7.
- Zdunek, K., & Karwat, T. (1996). Distribution of magnetic field in the coaxial accelerator of impulse plasma. *Vacuum*, *47*(11), 1391–1394. DOI: 10.1016/S0042-207X(96)00180-7.
- Garkusha, I. E., Cherednychenko, T. N., Ladygina, M. S., Makhlay, V. V., Petrov, Yu. V., Solyakov, D. G., Staltsov, V. V., Yelisyeyev, D. V., & Hassanein, A. (2014). EUV radiation from pinching discharges of magnetoplasma compressor type and its dependence on the dynamics of compression zone formation. *Phys. Scr. T*, *161*, 014037. DOI: 10.1088/0031-8949/2014/T161/014037.
- Solyakov, D. G., Petrov, Y. V., Garkusha, I. E., Chebotarev, V. V., Ladygina, M. S., Cherednichenko, T. N., Morgal', Ya. I., Kulik, N. V., Staltsov, V. V., & Eliseev, D. V. (2013). Formation of the compression zone in a plasma flow generated by a magnetoplasma compressor. *Plasma Phys. Rep.*, *39*, 986–992. DOI: 10.1134/S1063780X13110081.
- Bandura, A. N., Byrka, O. V., Garkusha, I. E., Ladygina, M. S., Marchenko A. K., Makhlay, V. A., & Tereshin, V. I. (2011). Characteristics of plasma streams and optimization of operational regimes for magnetoplasma compressor. *Probl. Atom. Sci. Techn.*, *1*(17), 68–70.
- Cherednychenko, T. N., Garkusha, I. E., Chebotarev, V. V., Solyakov, D. G., Petrov, Yu. V., Ladygina, M. S., Eliseev, D. V., & Chuvilo, A. A. (2013). Local magnetohydrodynamic characteristics of the plasma stream generated by MPC. *Acta Polytech.*, *53*(2), 131–133. DOI: 10.14311/1733.
- Ladygina, M. S., Marchenko, A. K., Solyakov, D. G., Petrov, Yu. V., Makhlay, V. A., Yelisyeyev, D. V., Garkusha, I. E., & Cherednichenko, T. N. (2016). Dynamics of self-compressed argon and helium plasma streams in the MPC facility. *Phys. Scr.*, *91*(7), 074006. DOI: 10.1088/0031-8949/91/7/074006.

9. Astashynski, V. M., Bakanovich, G. I., Kuz'mitskii, A. M., & Min'ko, L. Ya. (1992). Choice of operating conditions and plasma parameters of a magneto-plasma compressor. *J. Eng. Phys. Thermophys.*, *62*(3), 386–390. DOI: 10.1007/BF00851755.
10. Giovannini, A. Z., Barendregt, I., Haslinde, T., Hubbs, C., & Abhari, R. S. (2015). Self-confined plasma in a magneto-plasma compressor and the influence of an externally imposed magnetic field. *Plasma Sources Sci. Technol.*, *24*, 025007. DOI: 10.1088/0963-0252/24/2/025007.
11. Solyakov, D. G., Volkova, Yu. Ye., Ladygina, M. S., Merenkova, T. M., Marchenko, A. K., Garkusha, I. E., Petrov, Yu. V., Chebotarev, V. V., Makhlai, V. A., Kulik, M. V., Staltsov, V. V., & Yeliseyev, D. V. (2021). Distributions of magnetic field and current in pinching plasma flows: axial magnetic field effect. *Eur. Phys. J. Plus*, *136*, 566. DOI: 10.1140/epjp/s13360-021-01170-z.
12. Solyakov, D. G., Volkova, Yu. Ye., Garkusha, I. E., Marchenko, A. K., Ladygina, M. S., Staltsov, V. V., Petrov, Yu. V., Chebotarev, V. V., Merenkova, T. M., Lakhlai, V. A., & Yeliseyev, D. V. (2021). Measurement of the local electron temperature in self-compressed plasma stream. *Probl. Atom. Sci. Techn.*, *4*(134), 149–153. DOI: 10.46813/2021-134-149.
13. Baksht, F. G., & Rybakov, A. B. (1997). A theory of probes in high-pressure strongly-ionized plasmas. *Tech. Phys.*, *42*, 1385–1389. DOI: 10.1134/1.1258882.
14. Zhovtyansky, V. A., & Kolesnikova, E. P. (2013). The study of the near-wall layer in the dense plasma. *Probl. Atom. Sci. Techn.*, *1*(83), 240–242.
15. Zhovtyansky, V. A., Kolesnikova, E. P., Lelyukh, Y. I., & Goncharuk, Y. A. (2012). Peculiarities of heat and mass transfer processes in the near-wall region of dense plasma: Studies based on the use of electric probes. *Energy Technologies and Resource Saving*, *6*, 4–16. (in Russian).
16. Demidov, V. I., Ratynskaia, S. V., & Rypdal, K. (2002). Electric probes for plasmas: The link between theory and instrument. *Rev. Sci. Instrum.*, *73*(10), 3409–3439. DOI: 10.1063/1.1505099.
17. Popov, T. S. V. K., Dimitrova, M., Pedrosa, M. A., López-Bruna, D., Horacek, J., Kovačič, J., Dejarnac, R., Stöckel, J., Aftanas, M., Böhm, P., Bílková, P., Hidalgo, C., & Panek, R. (2015). Bi-Maxwellian electron energy distribution function in the vicinity of the last closed flux surface in fusion plasma. *Plasma Phys. Control. Fusion*, *57*(11), 115011. DOI: 10.1088/0741-3335/57/11/115011.